

Comparison of space weather effects of two major coronal mass ejections in late 2003^{*}

WANG Yu-ming, SHEN Cheng-long, YE Pin-zhong, WANG Shui

(CAS Key Laboratory of Basic Plasma Physics, School of Earth and Space Sci., USTC, Hefei 230026, China)

Abstract: Two similar major coronal mass ejections (CMEs) occurring on October 28 and November 18, 2003 were reported. Through the comparison of the two CMEs as well as their interplanetary responses, two primary space weather effects of them, i. e., solar energetic particle (SEP) events and large geomagnetic storms, were studied. The associated solar activities of both CMEs involved at least one large flare, a preceding minor fast CME and an eruption of filament. An extremely intense gradual SEP event was produced by the former CME, but no major SEP event appeared after the latter. However, they both caused a great geomagnetic storm and the storm created by the latter CME was slightly larger than the former. By analyzing observations of the two CMEs, their associated activities and the corresponding interplanetary magnetic clouds (MCs), the reasons why the two similar major CMEs caused different consequences in the geo-space were discussed. The difference between the two CMEs with respect to SEP events is due to the evident different release rate of energy, and the similarity and difference in geomagnetic storms are related to the MC orientations and the paths along which the Earth intersects the MCs.

Key words: coronal mass ejections; magnetic clouds; space weather; solar energetic particle events; geomagnetic storms

CLC number: P353 **Document code:** A

2003年10月与11月两次主要日冕物质抛射事件的空间天气效应比较

汪毓明, 申成龙, 叶品中, 王水

(中国科学技术大学地球和空间科学学院, 中国科学院基础等离子体物理重点实验室, 安徽合肥 230026)

摘要: 研究了分别发生在2003年10月28日和2003年11月18日的两次相似的强烈日冕物质抛射(CME)事件. 通过比较这两次CME事件以及它们的行星际响应, 分析了其伴随的两种主要空间天气效应: 太阳高能粒子事件和地磁暴. 这两次CME事件均伴随有一个强耀斑和一次暗条爆发, 并且之前都有一个较弱的CME从同一源区产生. 第一个CME事件引起了一次极大的太阳高能粒子事件, 而第二个则没有引起明显

* **Received:** 2007-03-02; **Revised:** 2007-06-10

Foundation item: Supported by NSF of China (40404014, 40336052, 40574063, 40525014), the startup fund of Chinese Academy of Sciences (KZCX2-SW-144), the China NKBRSF (973) Program (2006CB806304) and fund of the Ministry of Education of China (200530, NCET-04-0578).

Biography: WANG Yu-ming (corresponding author), male, born in 1976, PhD/Professor. Research field: Solar-terrestrial Physics and Space Weather. E-mail: ymwang@ustc.edu.cn

的太阳高能粒子事件, 这两次 CME 事件均引起了大的地磁暴, 且第二个 CME 所引起的地磁暴比第一个 CME 所引起的地磁暴更强. 通过比较分析这两次 CME 事件, 以及与之相关的活动现象和对应的行星际磁云 (MC), 讨论了这两次 CME 引起不同空间天气效应的原因: 形成不同强度的太阳高能粒子事件在于 CME 爆发过程中的能量释放率在这两次事件中显著不同, 而地磁暴强度的差异则是由行星际 MC 轴的方向以及 MC 经过地球时的相对位置不同造成的.

关键词: 日冕物质抛射; 磁云; 太阳高能粒子事件; 地磁暴; 空间天气

0 Introduction

Solar energetic particle (SEP) events and geomagnetic storms are two most important phenomena, known as the popular term “space weather effects”, in the geo-space. Coronal mass ejections (CMEs) are the main sources of them. However, not all of major solar CMEs can produce a gradual SEP event or a large geomagnetic storm.

The process of particle acceleration is very complicated. Shock wave acceleration is considered a main mechanism for the formation of gradual SEP events^[1,2]. Shock strength is the most important and substantial factor in energetic particle generations. Generally, interplanetary shocks are driven by fast CMEs. Statistical studies showed an evident association between CME speeds and SEP^[3]. Thus it is thought that a faster CME is more likely to produce an SEP event. However, there are still many other factors, such as CME longitude, interactions between multiple CMEs, background solar wind, seed populations, and so on, that affect the intensities of SEP events recorded near the Earth^[4~10]. Even with the presence of these factors, fast CMEs are not always able to produce an SEP event.

On the other hand, large non-recurrent geomagnetic storms are usually caused by interplanetary ejecta, especially magnetic clouds (MCs), and the shock sheaths preceding them^[11,12]. Fast solar winds (V), strong southward component (B_s) of magnetic fields and long duration of B_s (Δt) are the most pivotal to create large geomagnetic storms^[13]. In terms of the flux rope model of MC^[14,15], it is obvious that B_s and Δt are dependent on the orientation of the

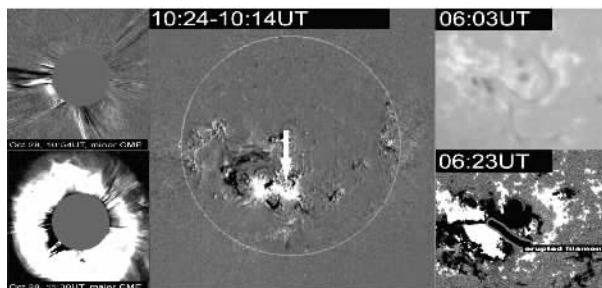
flux rope axis for a magnetic cloud. Therefore, the orientation of MCs is an important factor in geomagnetic storms. According to the recent work by Wang et al^[16], an MC can easily cause a large geomagnetic storm when its axis inclines southwards.

In this paper, we report two similar major coronal mass ejections occurring on October 28 and November 18, 2003, respectively, compare them as well as their associated activities and space weather effects, and try to answer the question of why they led to the similar and/or different consequences with respect to SEP events and geomagnetic storms. As will be represented in the following sections, the two CMEs and their associated activities are similar. Both the CMEs are halo and fast. They were both preceded by a minor CME. They were both accompanied with a large X-ray flare and a filament eruption. The interplanetary counterparts of both were clear magnetic clouds (MCs), which caused large geomagnetic storms. But one event produced a very intense SEP event, while the other did not. Thus, it is worth while to analyze the similarities and differences between the two major events for understanding of the solar-terrestrial physical processes. The following two sections present the observations of the two major CMEs as well as their associated phenomena.

1 Observations of CMEs and their associated solar activities

For convenience, the October 28 event is referred as I, and the November 18 event as II. Event-I has already been described in our previous paper^[17]. The CME first appeared in the field of

view (FOV) of LASCO/C2 at 11:30 UT on October 28, 2003. A bright Earth-directed full halo CME was moving out at an extremely fast speed of $>2\,000$ km/s (the left lower panel of Fig. 1). Based on the observations from SOHO/EIT (the middle panel of Fig. 1), it was found that the CME was associated with a violent X-ray flare (X17.2) occurring at S16E08 in AR 10486. The flare began at 09:51 UT and lasted until 11:24 UT with peak flux appearing at 11:10 UT. Simultaneously, a giant filament erupted. The main erupted part was in AR 10486 as marked by the white arrow. From the H_α and MDI observations shown in the right panels of Fig. 1, the erupted filament was approximately in northeast-southwest orientation. SOHO/MDI observations show that the observed longitudinal magnetic field was negative at the upper side of the filament channel and positive at the other side. This indicates that the coronal arcades overlying the filament directed from south-east to north-west roughly. During the interval of 24 hours centered on the occurrence of this CME, there was another small semi-halo CME appearing in the south-east in the FOV of LASCO at 10:54 UT (the left upper panel of Fig. 1). Compared to the 11:30 UT CME, this preceding CME was narrow (span angle was about 124°) and faint though its speed was higher



Running difference images of LASCO/C2 (left panels), running difference image of EIT195Å of the major CME (middle panel), the corresponding H_α image from Yunnan Astronomical Observatory (right upper panel) and the photospheric magnetic field observations of MDI (right lower panel). The white arrow marks the giant filament, which is denoted by the thick black line in the MDI image

Fig. 1 The solar observations of October 28 events

than 1000 km/s. This CME seemed to be also related to the X17.2 flare.

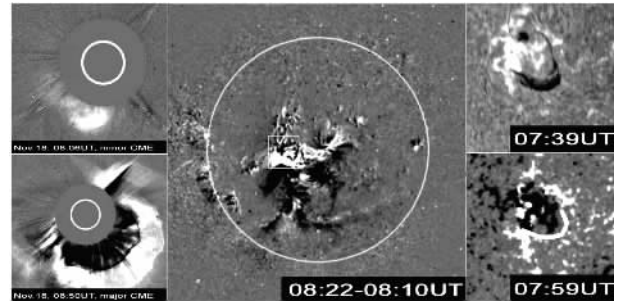


Fig. 2 Observations of the major solar activities on November 18

The CME of event-II first appeared in the southwest in the FOV of LASCO/C2 at 08:50 UT on November 18, and quickly extended over all directions (the left lower panel of Fig. 2). The estimated initial projected speed was $\sim 1\,660$ km/s, smaller than that of CME-I. This CME was associated with an M3.9 X-ray flare occurring at N00E18 in AR 10501 (as seen in the middle panel), which began at 08:12 UT and lasted until 08:59 UT with peak flux appearing at 08:31 UT. Before this CME, there was another small semi-halo CME appearing at 08:06 UT with an initial projected speed of $>1\,000$ km/s. It was related to an M3.2 flare from the same solar active region. In addition to the small CME, there was a limb CME occurring at 09:50 UT behind the southeast limb, which should not be taken into account in event-II. Similar to event-I, the CME was also accompanied with a thick prominence eruption in the AR 10501 (as shown in the right panels of Fig. 2). The H_α image show that the main part of the erupted filament was east-west orientation roughly. By combining MDI observations, it was found that the coronal arcades overlying the filament directed from south to north.

2 Consequences in geo-space

The interplanetary counterpart of CME-I passed the Earth from 11:00 UT on October 29 to 02:30 UT on October 30, which was recorded by the ACE spacecraft as seen in Fig. 3. Inside that

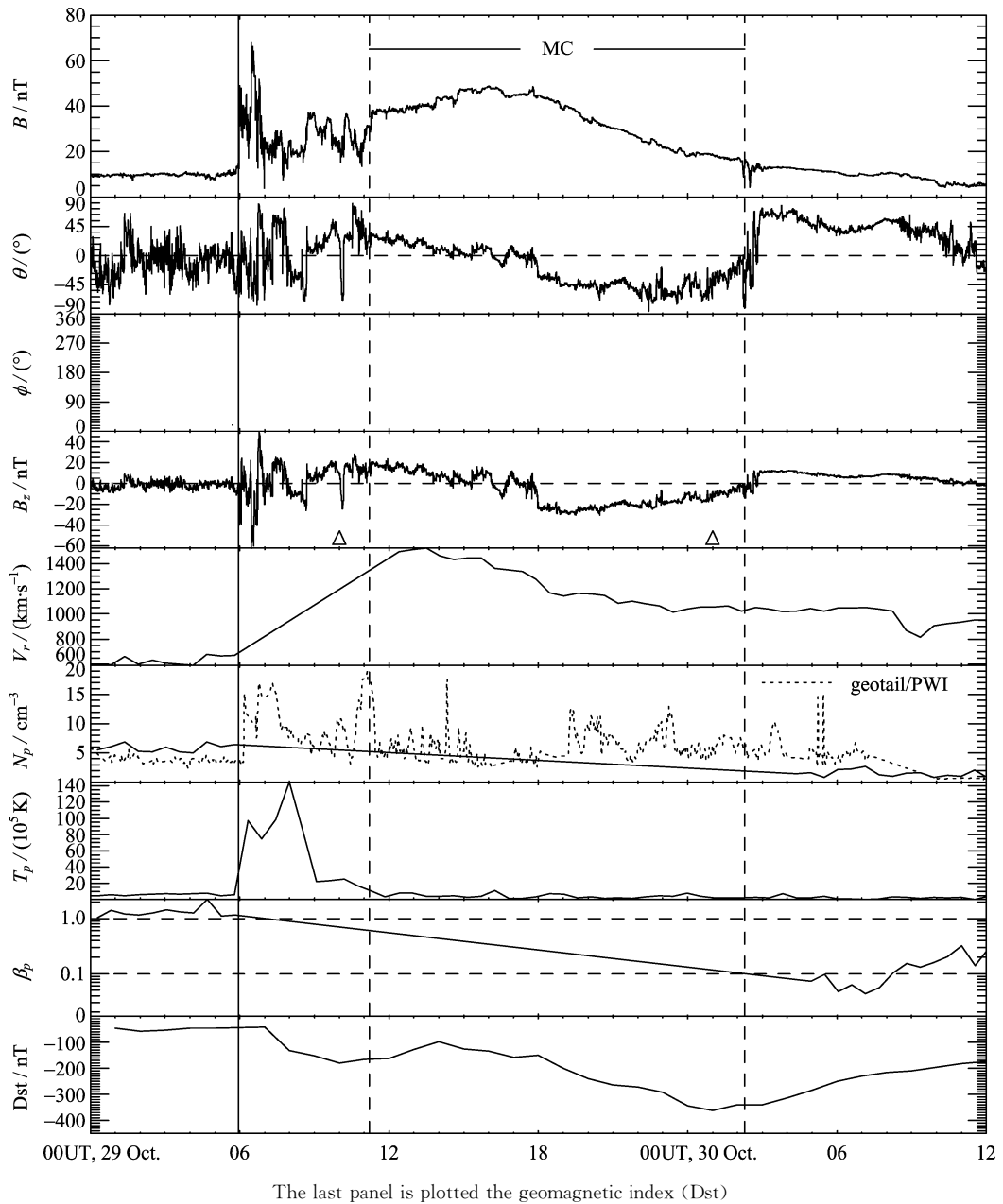
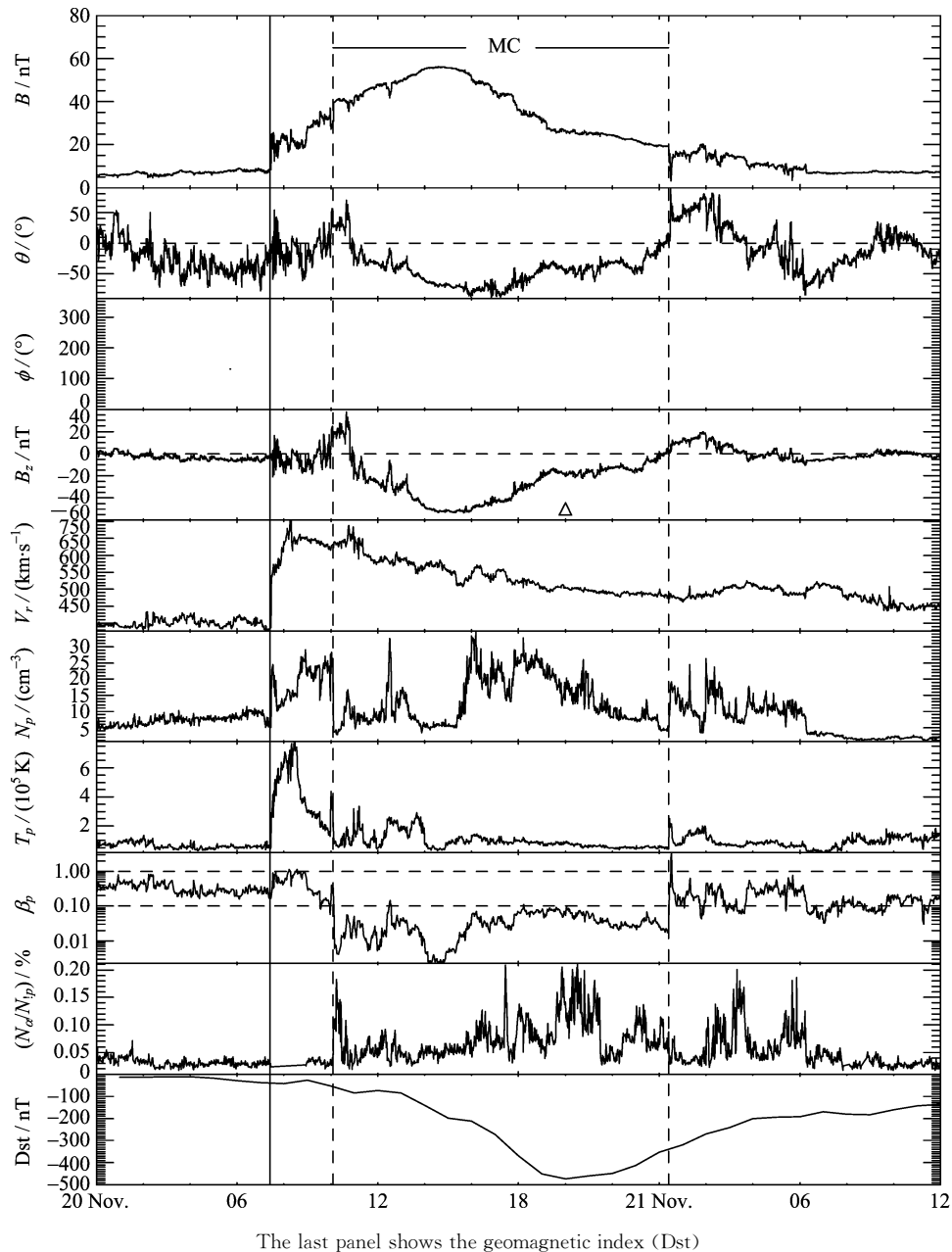


Fig. 3 The interplanetary observations of magnetic field strength (B), the elevation (θ) and azimuthal (ϕ) of field direction, the southward component (B_z) of magnetic field, solar wind speed (V_r), proton density (N_p), proton temperature (T_p), and the ratio of proton thermal pressure to magnetic pressure (β_p) from the ACE spacecraft

interval, the magnetic field strength was more intense than that in the ambient solar wind, the vector of the magnetic field rotated largely and smoothly, the proton temperature was relatively low, and the solar wind speed decreased continuously. These signatures suggest that the ICME was a definite magnetic cloud^[18]. Ahead of the cloud, a fast forward shock appeared at 06:00 UT, which was the strongest one in the late

October. Such fast shock implies a very fast moving magnetic cloud in the interplanetary medium. The average transit speed of the cloud from the Sun to 1 AU is estimated as 1 770 km/s approximately. Other halo or semi-halo CMEs occurring during October 26~28 were not likely to be the source of this cloud, because it is difficult for them to drive such a strong and fast shock^[17].

Similarly, the interplanetary counterpart of



The last panel shows the geomagnetic index (Dst)

Fig. 4 The interplanetary observations of magnetic field strength (B), the elevation (θ) and azimuthal (ϕ) of field direction, the southward component (B_z) of magnetic field, solar wind speed (V_r), proton density (N_p), proton temperature (T_p), the ratio of proton thermal pressure to magnetic pressure (β_p) and the density ratio of H_e^{++} to proton (N_a/N_p) from the ACE spacecraft

CME-II passed the Earth from 10:00 UT on November 20 to 00:30 UT the following day (Fig. 4). Except CME-II, there were no other halo or semi-halo CME from November 18 to 19. Thus the association between them is definite. This ejecta was also a clear magnetic cloud: enhancement of magnetic field strength, long and smooth magnetic field vector, low proton temperature, low proton

β , continuously declining of solar wind speed and relatively high density ratio of H_e^{++} to proton. The average transit speed of the cloud was ~ 850 km/s, much smaller than that of MC-I. This MC drove a fast shock at 07:30 UT on November 20. However, although the corresponding solar activities of event-II were relatively weaker than those of event-I, magnetic field strength (56 nT)

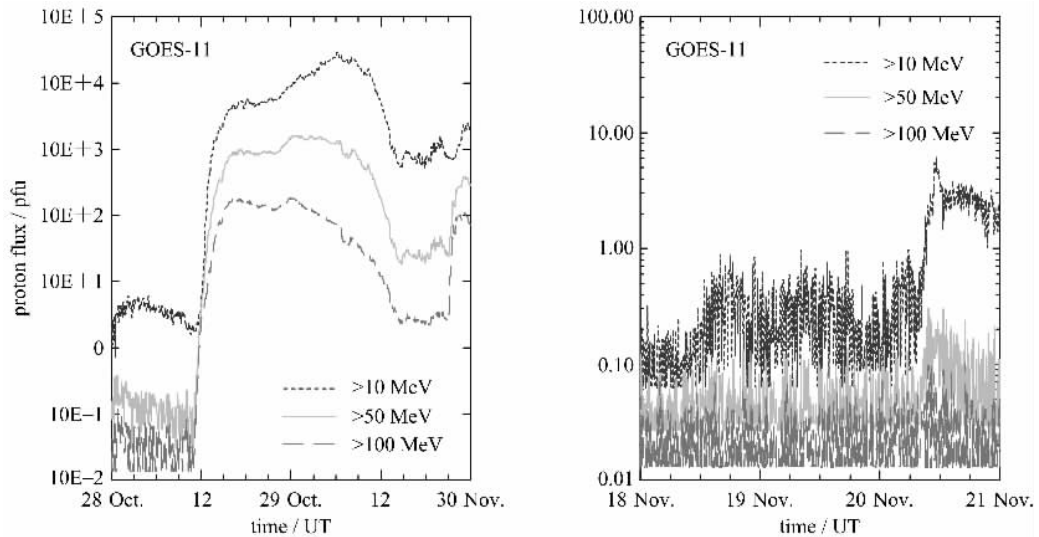


Fig. 5 SEP observations of GOES-11

observed in MC-II was intenser than that (49 nT) of MC-I.

The GOES observations show that an extraordinary intense SEP event was produced by event-I (the left panel of Fig. 5). The flux enhancement of the protons with energy >10 MeV started at 11:48 UT on October 28, and the flux reached up to the peak value of 29 500 pfu at 06:15 UT on the following day. On the contrary, event-II did not produce a major SEP event (the right panel of Fig. 5). There was merely a small enhancement of proton flux near the onset of CME-II, which did not exceed 1 pfu. The flux peak at $\sim 10:00$ UT was produced by another halo CME at 08:06 on Nov. 20.

By investigating the geomagnetic index, Dst, it was found that a great geomagnetic storm with Dst minimum value of -363 nT was caused by event-I. It began on the morning of October 29 and lasted until October 30. The bottom panel of Fig. 3 shows the Dst index of this storm. This storm contained a double-peak structure, which has been observed in previous work^[19,20]. The first peak (-180 nT) appeared at 10:00 UT on October 29, caused by the shock sheath ahead of the magnetic cloud. The southward component, B_s , of the magnetic field inside the sheath even reached up to ~ 60 nT. Although the duration of B_s was short, extremely large values of B_s played a

very important role in producing this Dst peak^[21]. The major Dst peak (-363 nT) appeared at 01:00 UT on October 30, produced by the long B_s intrinsic to the magnetic cloud. The magnitude of B_s was also large (30 nT), and the duration was much longer (>7 hours) than that of the B_s inside the shock sheath.

In spite of no major SEP event produced by event-II, a great geomagnetic storm with Dst minimum value of -472 nT was caused (the bottom panel of Fig. 4). The Dst index decreased largely from the arrival of MC-II-driven shock and reached the minimum at 20:00 UT on November 20. It was produced by the large and long B_s interval inside the cloud. The long B_s interval lasted more than half a day with the B_s peak value of 53 nT. It should be noticed that the peak value of B_s nearly reached the total magnetic field strength, i. e., the field almost directed southward totally, which implies that this MC was in favor of causing larger geomagnetic storms. The shock sheath did not create a small Dst peak due to the presence of neither extraordinary intense B_s nor long duration of B_s .

3 Summary and discussion

Two important geo-space effects (solar energetic particle event and geomagnetic storm) caused by the two large CMEs occurring in 2003 are analyzed. Although the two CMEs were similar

to each other, their consequences in geo-space were not similar. As a comparison, Tab. 1 clearly lists the two CMEs, their associated solar activities and their main interplanetary consequences. Both events involved at least one large solar flare, two CMEs (the major one was halo and large, and the minor one was relatively narrow and weak), and one evident filament eruption. The two CMEs in each event were both frontside and separated by nearly half an hour, indicating very that they were close in time. Nevertheless, they did not form multiple-magnetic-cloud structures^[22,23] or complex ejecta^[24], as the data from the ACE spacecraft suggests that there was only an isolated magnetic cloud observed for both October 28 and November 18 events. We consider that the most possible fate for the minor CMEs is that they had been pushed to a side and even did not pass through the Earth. Such phenomena could be termed “CME deflection”^[25,26].

Why did the two CMEs produce totally different SEP events in intensity though they were so similar to each other? According to the observations described above, the main differences between event-I and event-II are as follows. (I) Both the projected speeds and estimated transit speeds indicate that CME-I was significantly faster than CME-II, meaning that the shock driven by CME-I was stronger; (II) flare-I was much more intense than flare-II though they both belong to large flare. Moreover, the records of type II

radio bursts (as listed in the 7th column of Tab. 1) by Wind/Waves also suggest that CME-I drove a very strong shock but CME-II did not. These differences all imply that the process of the energy release of CME-I was much faster than that of CME-II. On the other hand, the two major CMEs both originated from the vicinity of the solar center meridian. The effect of the CME longitude on the intensities of SEP events^[4,5] can be ignored. Thus the most probable main explanation of why the two major CMEs did not cause similar SEP consequences is that CME-I released energy much more quickly than CME-II. Such a rapid release of energy made flare-I very large and CME-I driven shock very strong.

Although CME-I released energy much more quickly than CME-II, it does not follow that the amount of magnetic field fluxes ejected by CME-I was larger than that by CME-II. The two CMEs both formed MCs and caused great geomagnetic storms. As mentioned in Introduction, the orientation of MC's axis influences the strength of a geomagnetic storm. Wang et al^[16] have studied the orientation effect by analyzing 20 clear magnetic clouds associated with moderate to intense geomagnetic storms during 1998~2003. They suggested that large storms tend to occur when the elevation angle θ of a MC's axis with respect to ecliptic plan is less than zero, particularly when it is $< -45^\circ$. The two MCs

Tab. 1 Comparison of the two major events

No.	CMEs	Flares			EPs ^b	Type II ^c	MCs				Dst /nT	SEPs /pfu
		Time ^a /UT	Class	Loc			V_t^d (Km · s ⁻¹)	B_{max} /nT	$B_{s\ max}$ /nT	Δt /h		
I	appeared at 11: 30 UT, $V_i=2\ 459$ km/s, a preceding minor CME appeared 36 minutes before	09:51-11:10-11:24	X17.2	S16E08 AR486	Yes	Strong	1 770	49	30	>7	-363	29 500
II	appeared at 08: 50 UT, $V_i=1\ 660$ km/s, a preceding minor CME appeared 44 minutes before	08:12-08:31-08:59	M3.9	N00E18 AR501	Yes	Weak	850	56	53	>12	-472	<1

[Note] ^a Begin Maximum End of flares; ^b Eruption of prominences; ^c Type II radio bursts from <http://lep694.gsfc.nasa.gov/waves/waves.html>; ^d Transit speed of MCs from the Sun to 1 AU.

represented here is included in their sample. By using the force-free flux rope model^[14,15], the observed MCs are fitted as indicated by the solid curves in Fig. 6 and Fig. 7, and the fitted parameters are listed in Tab. 2. The fitting results suggest that the orientation (θ, ϕ) of the axis of the MCs were $(-12^\circ, 246^\circ)$ and $(-70^\circ, 90^\circ)$, respectively. They were in the range where a cloud may create a moderate to large geomagnetic storm.

Particularly, according to Wang et al^[16] results, MC-II is more apt to cause a great storm, as its axis directed to about -70° in θ . This is a reason why the storm caused by MC-II was larger than that by MC-I though CME-II was slightly weaker than CME-I. Besides, there is another more important reason that, compared to MC-I, the observational path of the spacecraft for MC-II was closer to the axis of the cloud, where the

magnetic field strength was relatively larger. The distance between the observational path and the axis of MC-I was estimated as $\sim 0.5R_0$ and that of MC-II was ~ 0.0 , where R_0 denotes the radii of the clouds. The fact that the width of the shock sheath ahead of MC-II was less than that ahead of MC-I seems to support this point of view, as a shock plane is farther away from its driver at the flank than at the nose. Thus, the geoeffectiveness of MC-II is more significant than that of MC-I. In addition, the above analysis implies that the effect of the rate of energy release of CMEs on geomagnetic storms is weak.

Acknowledgments: We acknowledge the use of the data from the SOHO, ACE, GOES spacecraft, the H_α images from the YNAO and KSO, and the Dst index from World Data Center. We thank Dr Skoug R, Dr Terasawa T, Dr Zurbuchen T,

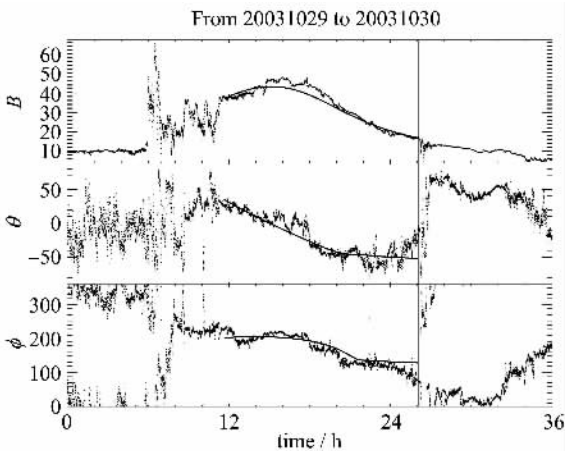


Fig. 6 The fitting results of the October magnetic cloud in GSM coordinates^[16]

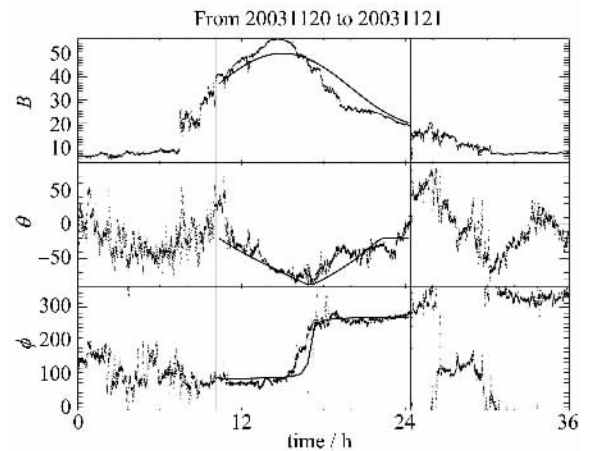


Fig. 7 The fitting results of the November magnetic cloud in GSM coordinates

Tab. 2 The two magnetic clouds and fitted parameters

No.	Date	Observations							Fitted parameters					
		t^a	V^b	n^c	B	B_s^d	B_\parallel^e	H^f	θ^g	ϕ^h	t_c^i	R^j	D^k/R	χ^2/cc^l
I	2003. 10. 29-30	11. 4-26. 1	1 200	6. 0	49	30	52. 5	-1	-12	246	15	6. 5	0. 508	0. 038/0. 95
II	2003. 11. 20-21	10. 1-24. 4	589	13. 4	56	53	50. 0	1	-70	90	15	7. 2	0. 0	0. 064/0. 95

【Note】 ^aStart and end of a magnetic clouds (hours); ^bAverage speed of a magnetic clouds (in km/s); ^cNumber density of solar wind plasma within a magnetic cloud (in cm^{-3}); ^dMaximum of southward component of magnetic field inside a magnetic cloud (in nT); ^eMagnetic field magnitude at the axis of a flux ropes (in nT); ^fSign of helicity of a flux rope, i. e., handedness; ^gElevation angle of axial field (i. e., axis) of a flux rope in GSM coordinates; ^hAzimuthal angle of axial field (i. e., axis) of a flux rope in GSM coordinates; ⁱCenter time at the closest approach to the cloud's axis; ^jRadius of a flux rope (in hours); ^kThe closest distance to the axis of a flux rope (in hours); ^lGoodness-of-fit, RMS deviation/correlation coefficient.

and Dr Raines J for providing the best available solar wind plasma data collected during October 29 ~30. We also thank Dr Zhou G P for preparing parts of Fig. 1 and Fig. 2.

References

- [1] Reames D V. Particle acceleration at the sun and in the heliosphere[J]. *Space Sci Rev*, 1999,90: 413-491.
- [2] Kallenrode M B. Current views on impulsive and gradual solar energetic particle events[J]. *J Phys G: Nucl & Particle Phys*, 2003,29:965-981.
- [3] Reames D V. Particle acceleration by CME-driven shock waves[C]//Invited, Rapporteur, and Highlight Papers, volume 516 of AIP Conf Proc, 2000:289-300.
- [4] Cane H V, Reames D V, Von Roseninge T. The role of interplanetary shocks in the longitude distribution of solar energetic particles[J]. *J Geophys Res*, 1988,93: 9 555-9 567.
- [5] Reames. D V. Energetic particles and the structure of coronal mass ejections[M]//Coronal Mass Ejections. *Geophys Monogr Ser*, 99, 1977:217-226.
- [6] Kahler S W. The correlation between solar energetic particle peak intensities and speeds of coronal mass ejections; Effects of ambient particle intensities and energy spectra[J]. *J Geophys Res*, 2001,06(A10): 20 947-20 955.
- [7] Kahler S W, Reames D V. Solar energetic particle production by coronal mass ejection-driven shocks in solar fast-wind regions[J]. *Astrophys J*, 2003, 584: 1 063-1 070.
- [8] Kahler S W. Solar fast-wind regions as sources of shock energetic particle production[J]. *Astrophys J*, 2004, 603:330-334.
- [9] Gopalswamy N, Yashiro S, Krucker S, et al. Intensity variation of large solar energetic particle events associated with coronal mass ejections[J]. *J Geophys Res*, 2004,109, A12105.
- [10] Shen C L, Wang Y M, Ye P Z, et al. Strength of coronal mass ejection-driven shocks near the sun, and its importance in prediction of solar energetic particle events[J]. *Astrophys J*, 2007, accepted.
- [11] Sheeley N R, Jr Howard R A, Koomen M J, et al. Coronal mass ejections and interplanetary shocks[J]. *J Geophys Res*, 1985,90(A1):163-175.
- [12] Gosling J T, McComas D J, Phillips J L, et al. Geomagnetic activity associated with earth passage of interplanetary shock disturbances and coronal mass ejections[J]. *J Geophys Res*, 1991, 96:7 831-7 839.
- [13] Gonzalez W D, Joselyn I A, Kamide Y, et al. What is a geomagnetic storm? [J]. *J Geophys Res*, 1994, 99: 5 771-5 792.
- [14] Burlaga L F. Magnetic clouds and force-free field with constant alpha[J]. *J Geophys Res*, 1988, 93: 7 217-7 224.
- [15] Kumar A, Rust D M. Interplanetary magnetic clouds, helicity conservation, and current-core flux-ropes[J]. *J Geophys Res*, 1996, 101:15 667-15 684.
- [16] Wang Y M, Ye P Z, Wang S. The dependence of the geoeffectiveness of an interplanetary flux rope on its orientation, with possible application to geomagnetic storm prediction[J]. *Sol Phys*, 2007, 240:373-386.
- [17] Wang Y M, Ye P Z, Zhou G P, et al. The interplanetary responses to the great solar activities in late October 2003[J]. *Sol Phys*, 2005, 226:337-357.
- [18] Burlaga L, Sittler E, Mariani F, et al. Magnetic loop behind an interplanetary shock; Voyager, Helios, and IMP 8 observations [J]. *J Geophys Res*, 1981, 86 (A8):6 673-6 684.
- [19] Kamide Y, Yokoyama N, Gonzalez W D, et al. Two-step development of geomagnetic storms[J]. *J Geophys Res*, 1998,103:6 917-6 922.
- [20] Jordanova V K, Kistler L M, Thomsen M F, et al. Effects of plasma sheet variability on the fast initial ring current decay[J]. *Geophys Res Lett*, 2003, 30 (6). 1 311,doi:10.1029/2002GL016,576.
- [21] Wang Y M, Shen C L, Wang S, et al. An empirical formula relating the geomagnetic storm's intensity to the interplanetary parameters: $-\overline{VB}_z$ and Δt [J]. *Geophys Res Lett*, 2003, 30(20). 2 039,doi:10.1029/2003GL017,901.
- [22] Wang Y M, Wang S, Ye P Z. Multiple magnetic clouds in interplanetary space[J]. *Sol Phys*, 2002, 211:333-344.
- [23] Wang Y M, Ye P Z, Wang S. Multiple magnetic clouds; Several examples during March-April, 2001 [J]. *J Geophys Res*, 2003,108(A10). 1 370,doi:10.1029/2003JA009850.
- [24] Burlaga L F, Plunkett S P, Cyr O C St. Successive CMEs and complex ejecta[J]. *J Geophys Res*, 2002, 107. 1 266,doi:10.1029/2001JA000255.
- [25] Wang Y M, Shen C L, Ye P Z, et al. Deflection of coronal mass ejection in the interplanetary medium[J]. *Sol Phys*, 2004, 222:329-343.
- [26] Wang Y M, Shen C L, Wang S, et al. Deflected propagation of coronal mass ejections in the interplanetary medium[C]//The 36th COSPAR Scientific Assembly, Beijing, China, 2006. COSPAR.